Study on backscattering from fish school near pump intake

Ling Fei Liu

NTNU

Fakultet for ingeniørvitenskap og teknologi
Institutt for marin teknikk

TMR 4905 – Master Thesis Marine Systems - spring 2013

Student: Lingfei Liu

Study on backscattering from a fish school near pump intake

Background:
The production environment for salmon fish farming is large sea-based cages with a diameter of typical 50 meters and one cage containing up to 1000 tons of fish. Well boats load live fish into water filled holds for operations like delousing, sorting or harvesting. The fish transfer is performed by using a hose between cage and boat, and the fish is pumped into the well boat. A crowding net is used to increase the density of the fish in front of the pump intake, and the fish density is controlled by reducing the volume of the net, which in turn is important for the fish pump rate. However, today no state of the instrumentation exists for measurement of the fish density in front of the hose intake, so farmers adjust the fish biomass intuitively based on their experience, which makes the pump rate control a challenging task for the operator.

Objective:
In this master project, acoustic methods will be applied for estimating the gradually changed fish density during the crowding near the pump intake in salmon cages. The purpose is to detect if the sensitivity of the echo sounder is feasible for density estimation.

Scope of Work:
The candidate shall perform the following main activities:

1. Conduct experiments at the Salmar Innovamar harvesting and processing plant with two 200 kHz single beam echo sounder Simrad EK15. The experiments shall include one normal group performed during the twice harvesting operations and one control group done after the harvesting for a nearly empty cage.
2. Process experimental data by use of Matlab and compare the results from the normal and control group.
3. Evaluate the acoustic results by comparing the backscattering strength (power) from fish school with the harvesting operation.

General:
The work shall be carried out and reported in accordance with guidelines, rules and regulations pertaining to the completion of a Master Thesis in engineering at NTNU.

The work shall be completed and delivered electronic by: June 10th, 2013.

Norges teknisk-naturvitenskapelige universitet

Main advisor is Professor Harald Ellingsen, Department of Marin Technology, NTNU.
Co-advisor is Professor Hefeng Dong, Department of Electronics and Telecommunications, NTNU.

Trondheim, February 27th, 2013

Harald Ellingsen

Abstract

In this master project, acoustic method was applied for estimating the gradually changed fish density during the crowding near the pump intake in salmon plant. The purpose was to detect if the sensitivity of the echo sounder is feasible for density estimation. The experiment was conducted at the Salmar Innovamar harvesting and processing plant with two 200 kHz single beam echo sounder –Simrad EK15. Two transducers holding by plates were used to collect the acoustic data. The distance between the plates was set as 4, 3, 2.5 and 1.5m, respectively. The experiment consisted of two parts: the first one was a normal group including two tests conducted during two harvesting periods; the second one was a control test that was done after harvesting in a nearly empty cage.

Raw data from the echo sounder were processed by Matlab to extract the power data without range compensation. There were some features of the acoustic results which can be explained with the harvesting operation log. However, the fish density was so great that the acoustic energy was decreased rapidly within a range of 2m, thus it is hard to connect the distribution of power with fish density within the sample volume. Additionally, the volume of the netting was always changed manually and it was impossible to quantify the real density.

Preface

This report has been written as the thesis for TMR4905 –Marine system at the Department of Marine Technology in the Norwegian University of Science and Technology (NTNU) spring 2013. This project focus on backscattering from fish school near pump intake and based on the idea of acoustic concept for aquaculture operation from SINTEF Fisheries and Aquaculture. The echo-sounder is provided by Sintef Fisheries and Aquaculture and the experiment was conducted on April, 18th at InnovaMar, SalMar.

I would like to thank my supervisors Prof. Harald Ellingsen (harald.ellingsen@ntnu.no) in the Department of Marine Technology for arranging group meetings and Prof. Hefeng Dong (hefeng.dong@iet.ntnu.no) in the Department of Electronics and Telecommunications who gives me the knowledge of fishery acoustic and I am grateful for her guidance and support throughout the whole project. I am thankful for Kevin Frank and Per Rundtop at Sintef Fisheries and Aquaculture giving me the idea of this work. I would like to thank Kevin for his great help and guidance including the design of the experiment, pre-test of the equipment, experiment on site, signal process and data analysis. I would like to thank Torbjørn Hammernes, Thomas Sandvik, Tomsz Trzaska and Peter Petrov at InnovaMar, SalMar for providing me a lot of great information of the plant, the harvesting operation and salmon, and help me to set up the equipment and participate in the whole experiment. I would like to thank Frank Reier Knudsen from Simrad for the guidance on the setup and use of the echo-sounder. I would like to thank Kristin Johansen Mørkve and Trond Inndet at the Department of Marine Technology making the two wooden plates for the experiment. I would like to thank all my friends and fellow students for the great time in the university. I would like to thank my family and my dear Fiancé Mingming Hui, you mean the world to me.

A special thank to Prof.Yingqi Zhou in Shanghai Ocean University and Prof. Yngvar Olsen in Department of Biology, NTNU for their encouragement for applying a master degree in NTNU and the scholarship for these two years. This opportunity is so important for my life.

Lingfei Liu

Contents

List of figures

List of tables

1 Introduction

Aquaculture is one of the most important industries for supplying food. In Norway, Farmed Atlantic salmon has accounted for more than 80 percent of the total Norwegian aquaculture production (FAO, 2012). Farmed salmon is a healthy product for the marine omega-3 polyunsaturated fatty acids eicosapentaenoic acid (EPA) and docosahexaenoic acid (DHA) that reduce the risk for cardiovascular disease. Protein production efficiency is really high for farmed salmon compared with other protein productions, such as cattle, pork, and poultry (Marine harvest, 2012). As a result of the growth of the global population and the limitation of fresh water, aquaculture industry should be expanded in the future.

1.1 Motivation

The production environment for salmon fish farming is large sea-based cages with a diameter of typical 50 meters and one cage contains up to 1000 tons of fish. Well boats loads live fish into water filled holds for operations like deicing, sorting or harvesting. The fish transfer is performed by using a hose between cage and boat, and the fish is pumped into the well boat.

A crowding net is used to increase the density of the fish in front of the hose inlet, and the fish density is controlled by reducing the volume of the net, which in turn is important for the fish pump rate. It is important to optimize the pump rate in order to reduce the time for fish loading and to ensure fish welfare.

Fish behavior will be greatly impacted by the operation and lead to great inhomogeneous distribution of fish density in the crowding net. For instance, a high density near the hose due to the pumping. Additionally, many fish will gather near the edge of the crowding net due to being frightened from the changing surrounding water and noise from the well boat or pumping. Too high density will cause the problems of dead fish and broken net, but the low density makes the operation low efficiency and energy consuming.

However, today no state of the art instrumentation exists for measurement of the fish density in front of the hose intake and farmers always adjust the fish biomass intuitively

based on experience, which makes the pump rate control a challenging task for the operator.

Since acoustic technology has been used in fisheries industry for a long time, we would like to find a solution from acoustic concept to estimate the fish density near the pump intake.

In this project, two single-beam echo-sounders will be applied for estimating the gradually changed fish density during the harvesting operation near the pump intake in salmon plant. The purpose is to detect if the sensitivity of the echo sounder is feasible for density estimation. Additionally, two wooden plates used to hold the echo-sounders will be set with different distances to show the shadow effect of the high fish density.

1.2 Review of previously work

Acoustic instruments, such as single beam echo sounder, dual beam echo sounder and split-beam echo sounder are commonly used in fishery research either for fish detection or abundance investigation at sea. Typical frequencies of the echosounders used in fishery applications are 38 kHz, 120 kHz, 200 kHz or 420 kHz. (Simmonds and MacLennan, 2005). Multibeam technology has been developed and adapted to fish research, one example is DIDSON acoustic camera produced by Sound Metrics, which has high frequency up to 1.8 MHz.

The first acoustic technique for fish biomass estimation is echo counting, which is applied when individual targets are well separated and random distributed. The density of fish could be calculated by the count of these echoes within the acoustic beam. The size of targets could be determined from the amplitude of the echoes.

In the case of fish schooling, there are usually many targets at the same depth within the acoustic beam and the density is often too high for echo counting to estimate the fish abundance reliably. The alternative approach is echo integration, based on the linearity theory. The fish density could be obtained from the total acoustic energy of the whole school divided by the energy of an individual fish.

Acoustic research for fish in sea cage has been done for a long term, and mainly concerned with the correlation between target strength and fish length which can help to estimate the fish size (Knudsen, *et al*, 2004). However, good results for estimating the density distribution of fish school in cage are quite few. It is complicated problem because the high density will induce the high-order multiple scattering and shadow effect. The shadow effect is defined by the reduction of energy on the distant targets compared with the targets near the transducer (Zhao and Ona, 2003).

A relevant research was conduct with one multibeam and one split beam echo sounder for a group of Atlantic Cod in a submerge cage by Gurshin, *et al* (2009). Acoustic strength data were compared with the actual fish density which were changed from 1.31, 1.18, 0.67, and 0.23 fish per m^3, respectively. The measured data could describe the different spatial distribution when the density was sufficiently large or small, but failed to show the intermediate density. The mean volume-backscattering strength was not proportional to the actual fish biomass as expected from the linear echo-integration theory (Simmonds and MacLennan, 2005).

1.3 Structure of the report

- In chapter 1, introduce the background for this report and give a short review of acoustic scattering in fishery including acoustic measurements and acoustic scattering models.

- In chapter 2, represent the self-consistent model method which is based on air bubble model for fish schooling scattering; perform a simulation based on the self-consistent model for a salmon school; present results and discussions for the influences of frequency, azimuth and the deviation of fish location on schooling scattering in terms of target strength, respectively.

- In chapter 3, represent one experiment with two echo-sounders conducted in Salmon slaughtering plant; the experiment is including one normal group performed during the twice harvesting operations and one control group done after the harvesting for the nearly empty cage; show how the acoustic raw data is collected.

- In chapter 4, process the raw data with Matlab and the power data are chosen to show the backscattering strength from fish school in the sample volume; analyze how the power data are changed during the operation; evaluate the acoustic results by comparing their trends with the real operation.

- In chapter 5 and 6, describe discussion, future work and give conclusions.

1.4 Definitions
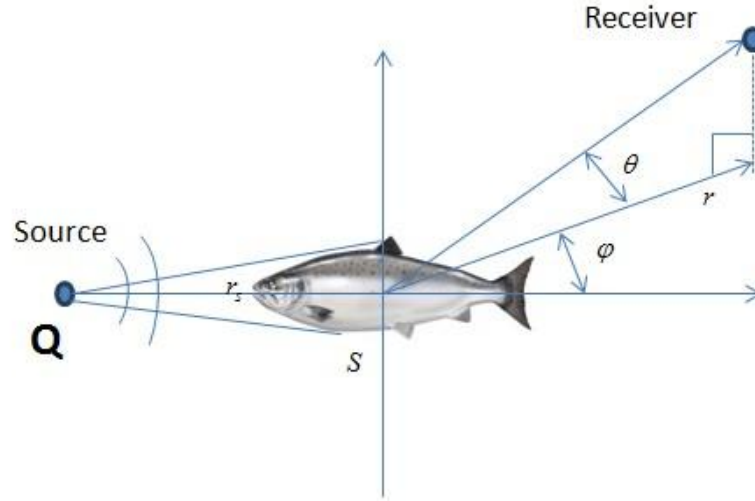
Figure 1: Echo measurement of a target with surface *S*. (Hovem, 2012)

A source with source strength Q is propagating spherically through a target with surface S at a distance r_s, the wave is scattered by the target and then received by a receiver at a distance r, in the direction indicated by φ and θ as shown in Figure 1.

All the definitions here are referred to Hovem (2012):

The incident field on the target, $\emptyset_i$ is

$$\emptyset_i = \frac{Q}{4\pi r_s} exp[i(kr_s cos\theta - \omega t)] \tag{1}$$

where Q is the source strength, k is the wave number defined by $k = \omega/c$, ω is the wave frequency and c is the sound speed in water.

The intensity of the incident wave is I_i; the scattering intensity per unit of solid angle is termed $I_s(\theta, \varphi)$, and the backscattering intensity is

$$I_{bs} = I_s(\theta = \pi, \varphi = 0) \tag{2}$$

The backscattering cross section could be expressed by:

$$\sigma_{bs} = r^2 \frac{I_{bs}}{I_i} \tag{3}$$

The total scattering intensity of the object is:

$$I_{tot} = \iint I_s(\theta, \varphi) d\Omega \tag{4}$$

The total scattering cross section is:

$$\sigma_s = r^2 \frac{I_{tot}}{I_i} \tag{5}$$

It is more common to use the sonar scattering cross section, σ in practice, which is defined by:

$$\sigma = 4\pi\sigma_{bs} \tag{6}$$

Then the target strength TS is:

$$TS = 10 \cdot log\left(\frac{\sigma}{4\pi}\right) \tag{7}$$

The volume backscattering coefficient, s_v, is a measure of echo intensity from a sampled volume, V_0, which contains many small individual targets.

$$s_v = \frac{\sum \sigma_{bs}}{V_0} \tag{8}$$

Then the volume backscattering strength can be expressed by:

$$S_v = 10\, log(s_v) \tag{9}$$

2 Theory

2.1 Scattering model for fish school

Theoretical model is developed for understanding the complex physical phenomenon of the scattering from fish schooling.

2.1.1 The Minnaert/Devin theory for one bladder

This theory was firstly calculated by Minnaert (1933) for gas bubble in water and then was further developed and applied for fish with a gas-filled swimbladder by Feuillade, *et al.* (1996,2001). Although the real shape of the bladder is normally a prolate elliptical, but many research have been confirmed that in models the spherical shape is good enough to show the scattering features of the fish and it is also much easier for calculation.

The spherical bubble has a radius a which has a value corresponding 5% of the body length and much smaller than the wave length. The viscous fluid is assumed to have the same density ρ and sound speed c as sea water.

The mechanism of the bubble scattering can be expressed by the perturbation of the bubble due to both the force from the external sound pressure and the ability of the bubble to balance the external force by its elasticity and dynamic force (Hovem, 2012).

Then based on these assumptions and theory, one mass spring type differential equation for the motion can be introduced to describe the scattering behavior of the bubble or bladder (Feuillade, *et al*, 1996):

$$m\ddot{v} + b\dot{v} + \kappa v = -Pe^{i\,\omega t} \tag{10}$$

where v is the differential volume which denotes the difference between the instantaneous and equilibrium bubble volumes caused by the sound pressure of the plane incident wave with amplitude P and frequency ω; the dynamic mass of the

bubble $m = \frac{1}{4}\rho\pi a$; b describes the damping of the bubble; $\kappa = 3\gamma P_a/4\pi a^3$ is the stiffness term, represents the bubble's elastic; γ represents the ratio of gas specific heats, P_a is the ambient pressure. This describes the Rayleigh scattering which means that the incident wave length should be much larger than the radius of the bladder (Hovem, 2012).

For a harmonic steady state, the solution of equation (10) can be in term of $\bar{v}e^{i\omega t}$, and then the radial pulsation amplitude is expressed by (Feuillade, *et al*, 1996):

$$\bar{v} = \frac{-P}{\kappa - \omega^2 m + i\,\omega b} = \frac{-P}{\left[\frac{\omega_0^2}{\omega^2} - 1\right] + i\frac{b}{m\omega}} \tag{11}$$

where the resonance frequency of the bubble is $\omega_0 = \sqrt{\kappa/m} = (\sqrt{3\gamma P_a/\rho})/a$; $\frac{b}{m\omega}$ can be identified as the attenuation coefficient $\delta(\omega)$,consisting of the radiation, viscosity and thermal effect:

$$\frac{b}{m\omega} = \delta(\omega) = \delta_r + \delta_v + \delta_t \tag{12}$$

where δ_r represents the attenuation caused by acoustic radiation, δ_v represents loss caused by viscosity and friction and δ_t represents thermal loss.

At resonance frequency, there has a typical way to describe the attenuation by one quality factor Q (Feuillade, *et al*, 1996):

$$\frac{b}{m\omega_0} = \delta(\omega_0) = \frac{1}{Q} \tag{13}$$

According to the research from Love (1978), the attenuation coefficient δ of fish swimbladder can be described by $\frac{\omega_0}{\omega H}$, where H is a frequency-dependent parameter, and also including three components as $\delta(\omega)$ in equation (12) (Feuillade, et al, 1996):

$$\frac{1}{H} = \frac{1}{H_r} + \frac{1}{H_v} + \frac{1}{H_t} \tag{14}$$

where the radiation term $H_r = \frac{\omega_0 c}{\omega^2 a}$; the viscosity term $H_v = \frac{\omega_0 \rho a^2}{2\xi}$, where ξ is the viscosity of fish; the value of thermal term H_t is negligible compared with the first two terms.

Finally, the acoustic field scattered by a bubble at distance r could be expressed by:

$$p(r) = \frac{\rho e^{-ikr}}{4\pi r} \ddot{v} = \frac{-\rho \omega^2}{4\pi r} \bar{v} e^{i(\omega t - kr)} = f \, P \frac{e^{i(\omega t - kr)}}{r} \; ; \tag{15}$$

where f is the scattering amplitude:

$$f = \frac{a}{\left[\frac{\omega_0^2}{\omega^2} - 1\right] + i\delta} \tag{16}$$

Until now this model is applied as the basic framework for the latter schooling scattering.

2.1.2 The self-consistent approach for bladders

The self-consistent approach is developed by Twersky (1962). In this method, when an external field with the amplitude P is propagating through a group of bubbles or bladders, the total scattering on one of the bladders has two contributions, one is directly from the external field, and the other is from other bubbles in terms of multiple scattering effects.
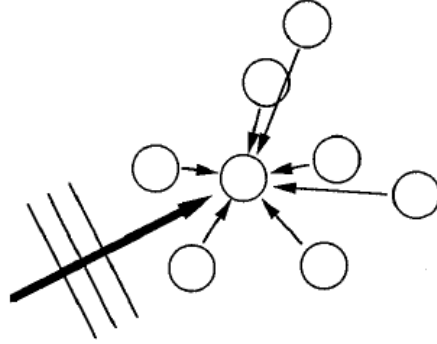
Figure 2: The self-consistent approach. (Feuillade, 1996)

Based on equations (10) and (15), the scattering behavior of one bladder in a group with N individuals can be expressed as follows (Figure 2) (Feuillade, *et al.*, 1996):

$$m_1 \ddot{v}_1 + b_1 \dot{v}_1 + \kappa_1 v_1 = -P_1 e^{i(\omega t + \phi_1)} - \sum_{j \neq 1}^{N} \frac{\rho e^{-ikr_{j1}}}{4\pi \, r_{j\,1}} \ddot{v}_j \;;$$

$$\ldots \ldots$$

$$m_n \ddot{v}_n + b_n \dot{v}_n + \kappa_n v_n = -P_n e^{i(\omega t + \phi_n)} - \sum_{j \neq 1}^{N} \frac{\rho e^{-ikr_{jn}}}{4\pi \, r_{j\,n}} \ddot{v}_j \;;$$

$$\ldots \ldots$$

$$m_N \ddot{v}_N + b_N \dot{v}_N + \kappa_N v_N = -P_N e^{i(\omega t + \phi_N)} - \sum_{j \neq 1}^{N} \frac{\rho e^{-ikr_{jn}}}{4\pi \, r_{j\,N}} \ddot{v}_j \qquad (17)$$

where *n* refers to an arbitrary individual in the school; P_n is the amplitude of the external field of the *n*th bladder; ϕ_n is the phase of the external field of the *n*th bladder ; $r_{j\,n}$ is the distance between the n individual and the other arbitrary individual *j*; m_n, b_n and κ_n has been described in section 2.1.1 and generally these are the same for all bladders if they have the similar dimensions and properties; the first term of the right hand side of the formula shows the force from the external field and the second term describes the multiple scattering inside the group. The method has completely shown the all the interactions both with the external field and internal of the school.

At the harmonic steady state, as shown for a single fish, the solution is in terms of $v = \bar{v}e^{i\omega t}$ which can be calculated by transferring equation (17) into a matrix form (Feuillade, *et al.*, 1996):

$$Mv = p \tag{18}$$

where $v = \{\overline{v_1}, \ldots, \overline{v_n}, \ldots \overline{v_N}\}$ and $p = \{-p_1 e^{i\,\phi_1}, \ldots, -p_n e^{i\,\phi_n}, \ldots, -p_N e^{i\,\phi_N}\}$ are the radial pulsation amplitude and external field for the N individuals. $\boldsymbol{M}$ term has two components with different properties:

$$M_{nn} = \kappa_n - \omega^2 m_n + i\,\omega b_n;$$

$$M_{nj} = \frac{-\omega^2 \rho e^{-i\kappa r_{jn}}}{4\pi r_{jn}} \ (n \neq j). \tag{19}$$

where M_{nn} indicate the diagonal terms in $\boldsymbol{M}$ matrix which describe the scattering behavior of one single bladder; They only depend on the individual characteristics of the bladders (size, damping, depth etc.); M_{nj} show the off diagonal terms which express the coupled effect between each two bladders and only depend on the spacing and distribution of individuals.

When applying this model in practice, the value of the amplitude of the external field on different bubbles in equation (17) should be considered carefully. For a dense and large fish school, the amplitude on the distant targets might be relatively weak compared with the targets near the source due to the shadow effect. But this problem can be simplified and avoided by applying the model for small schools (Feuillade, *et al*., 1996). Then after getting the solution of equation (18), the target strength of the fish schooling can be expressed by:

$$TS = 10\,log_{10}\left(\frac{\sigma_s}{4\pi}\right) = 10\,log_{10}\left(\frac{\omega^4 \rho^2 |\sum_{n=1}^{N} \overline{v_n}\,e^{i\,\phi_n}|^2}{(4\pi)^2 p^2}\right) \tag{20}$$

The self-consistent approach is able to describe the scattering of the school comprehensively and has a large range of suitable frequency. It is chosen for studying the scattering features of groups of salmon in the crowing net.

2.1.3 Simulation of the spherical scattering model for Atlantic salmon

The solution for the density distribution of salmon by acoustic concept in sea cage is not straightforward because it is too complex. An alternate way is to analyze how the variable distribution of fish density will affect the acoustic scattering level. And then some information of the density might be found indirectly.

In this section, the method described by Feuillade, *et al.* (1996) has been used. It is based on the self-consistent approach. The purpose is to show the basic scattering feature of a school of Atlantic salmon.

There are two assumptions for the simulations as Feuillade, et al (1996). First, the simulated school has a basic cubic structure with the edge of d as shown in Figure 3. The movement of fish can be shown by different deviations of fish locations ☐. The school contains 13 fish with the same body length. One fish is placed in the center of the cubic; eight fish are at the corners; then make the school in an approximately ellipsoidal shape which is more real as in natural by adding 4 fish at the front, the back, the up and the down side, respectively. Second, since the simulated school is small and with less indivuials, the amplitude of the external field on each individual is assumed to be the same and the attenuation of the scattering energy is neglected. So the equation (2.11) can be applied here.
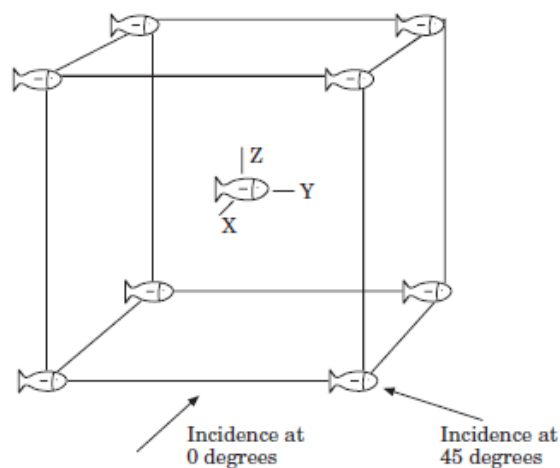
Figure 3: A diagram of a cubic school unit

According to the Marine Harvest hand book Salmon Farming Industry (2012), the average weight of fish for slaughtering is 4.5 Kg with body length around *L*=74 cm.

Swim bladder volumes are roughly 4%–5% of fish volumes (Feuillade, *et al.* ,1996), which corresponds to a bladder radius of about *a*=0.05*L*=3.7cm. The fish flesh viscosity is given the value ☐=500 poise (Feuillade, *et al.*, 1996) .Our main goal is about the fish distribution near the hose, so the water depth of the school is set to 0 m in all simulations. The school is assumed to be ensonified horizontally. The main parameters are shown in Table 1.

Table 1: Parameter values used for simulations.

Symbol	Name	Value
☐	Density of sea water	1026 kg/m3
☐	sound speed	1500 m/m3
☐$_☐$	Ambient pressure	1.01e5 Pa
☐	Ratio of gas specific heats	1.4
☐	Viscosity of fish flesh	500 poise
☐	Body length of salmon	0.74 m
☐	Swimbladder radius	0.037m

2.1.4 Results and discussions

In this section, the results of the simulations are given. The influences of frequency, azimuth and the deviation of fish location on schooling scattering in terms of target strength, are discussed, respectively. This model is valid for the Rayleigh scattering which means that the incident wave length should be much larger than the radius of the bladder (Hovem, 2012), so the largest frequency of the simulations is 5000Hz.
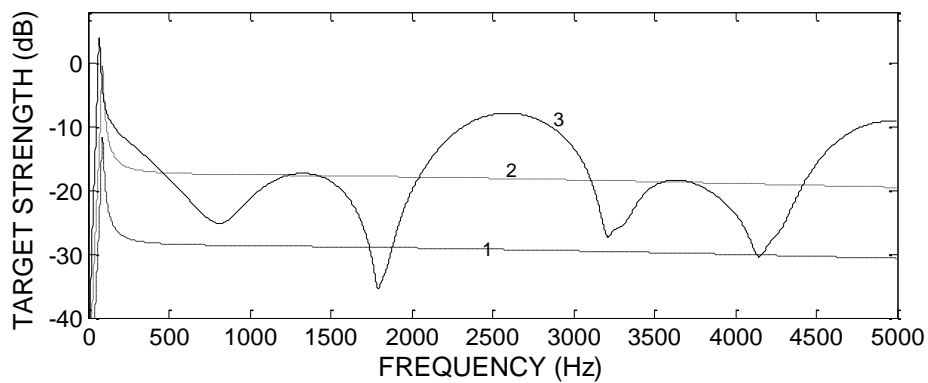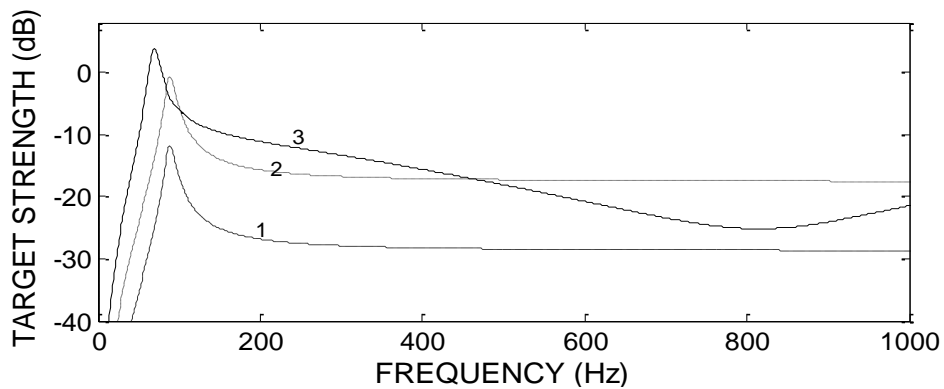
Figure 4: Scattering from a school with 13 fish. (a) Curve 1: Target strength of one fish; Curve 2: Target strength of 13 fish calculated from incoherent summation; Curve 3: Target strength of the school calculated by the self consistent model. (b) the same as (a) but the highest frequency is limited to 1000 Hz to show the change near the resonance frequency.

In Figure 4, curve 1 shows the target strength of a single fish. There is a peak around -12 dB at about 100 Hz which is the resonance frequency of the fish. The value of Curve 2 is calculated by the incoherent summation of the backscattering cross sections from the 13 fish in the school by assuming that there is no phase difference and no multiple scattering between the individuals.

Curve 3 shows the target strength calculated using the school scattering model with the

14

spacing $d = 60$ cm and $\sigma = 4$ cm. The result has some features. First, as shown in (b), the target strength of the school has a resonance peak at a lower frequency compared with the single fish.   Second, target strength of the school is unstable and oscillating with the incoherent summation as increased the frequency beyond resonance. The response is the result of the constructive and destructive effect of the scattered wave fields inside the school. These two features are agreed with Feuillade, *et al.* (1996). But the peak value of target strength at resonance is higher than the incoherent summation; however, the result of peak value is lower than the incoherent summation in Feuillade, *et al*. (1996). The reason for this inconsistent is unsure recently.

(2)Effect of Azimuth on fish school scattering
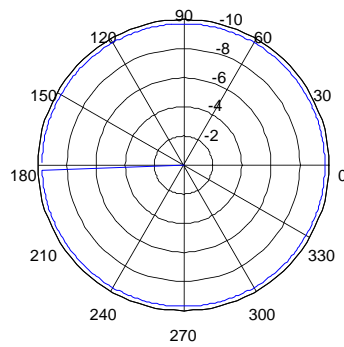
(a) *f*=50Hz
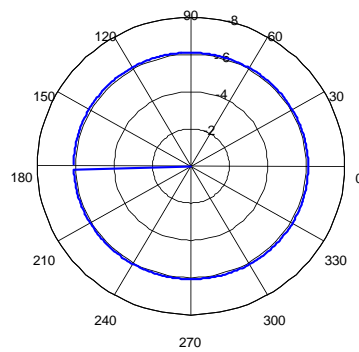
(b) *f*=100Hz
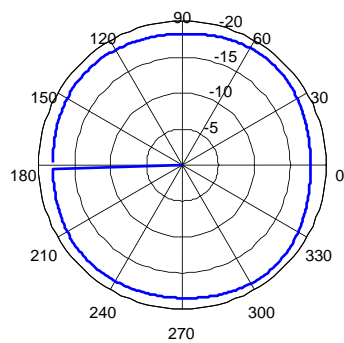
(c) *f*=500Hz
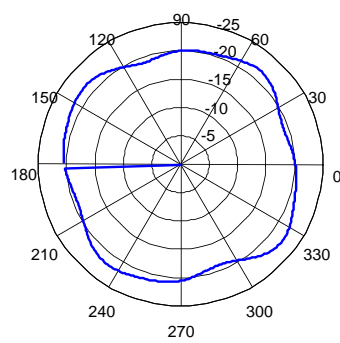
(d) *f*=1000Hz

(e) *f*=1500Hz   (f) *f*=5000Hz
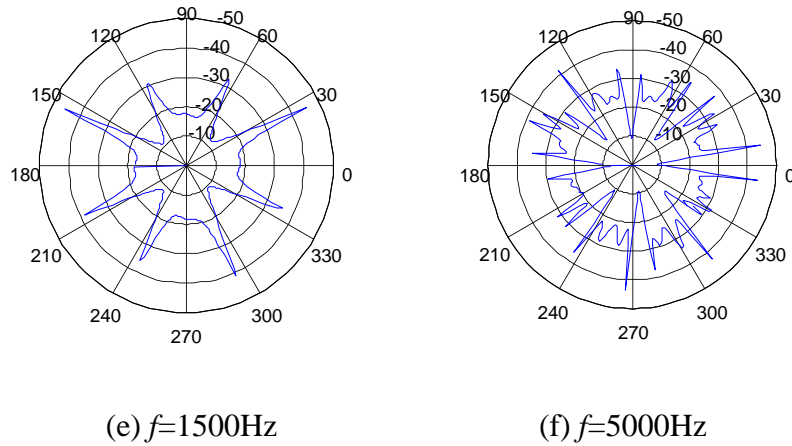
Figure 5: Effect of Azimuth on fish school scattering. (a) 50 Hz. The scattering is an isotropic distribution. (b) 100 Hz. The scattering is isotropic with an increase of target strength. (c) 500 Hz. The scattering is slightly asymmetric. (d) 1000 Hz. A trend to have lobes and nulls. (e) 1500 Hz. Several nulls and lobes appear. (f) 5000 Hz. The scattering is highly dependent on the azimuthal angle.

As shown in Figure 5, the school is always ensonified horizontally over 360 deg. The fish spacing and the deviation of location are maintained at $\square = 60$ cm and $\square = 4$ cm, respectively. Figure 8 (a) shows the azimuthal distribution of the target strength at 50 Hz, which corresponds to half of the resonance peak. At this frequency, the acoustic wavelength is about 30m. This is much greater than the separation between any two individuals in the school and about 50 times of the school dimension. As a result, the scattering field of the school is equal to the constructive summation of the 13 fish and leads to the isotropic distribution of the target strength with a value around -9.725 dB. The frequency is 100 Hz in Figure 5(b), which is near the resonance peak of school. The acoustic wavelength is about 15m, which is much greater than the dimension of the school. So the azimuthal scattering distribution is similar with (a) but the value has increased to about -6.1 dB.

When the frequency is increased to 500 Hz (c) and 1000 Hz (d), the distribution of target strength become slightly asymmetric and trend to have lobes and nulls, respectively. Figure 5 (e) shows the azimuthal distribution at 1500 Hz. Several nulls and lobes appear and the effect of azimuth is significant. Figure 5 (f) shows the azimuthal distribution at 5000 Hz. The acoustic wavelength is much smaller than the school dimension. The scattering is highly dependent on the azimuthal angle.

(3) Effect of different deviations of fish locations

(a) $\sigma = 4$ cm

(b) $\sigma = 8$ cm

(c) $\sigma = 16$ cm

17
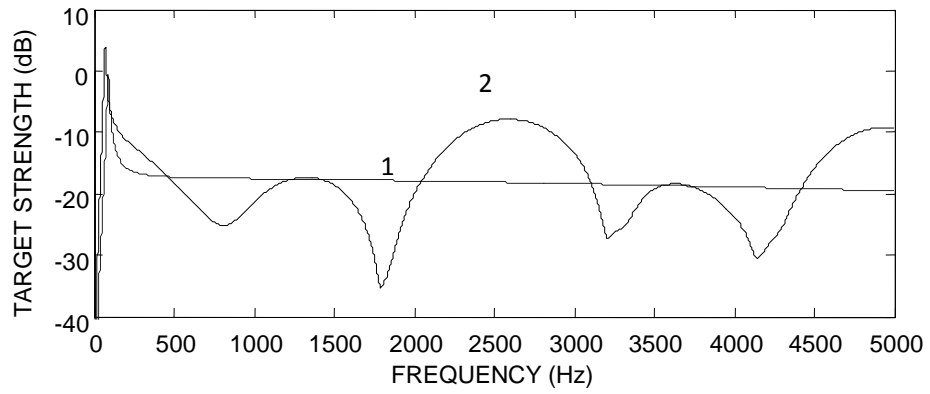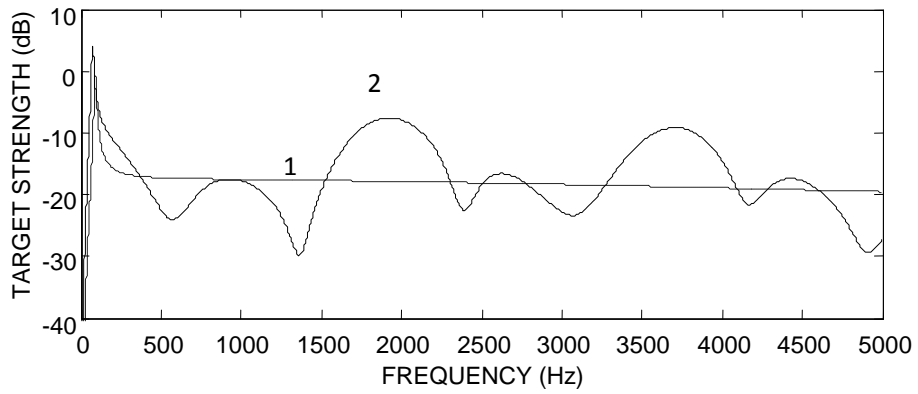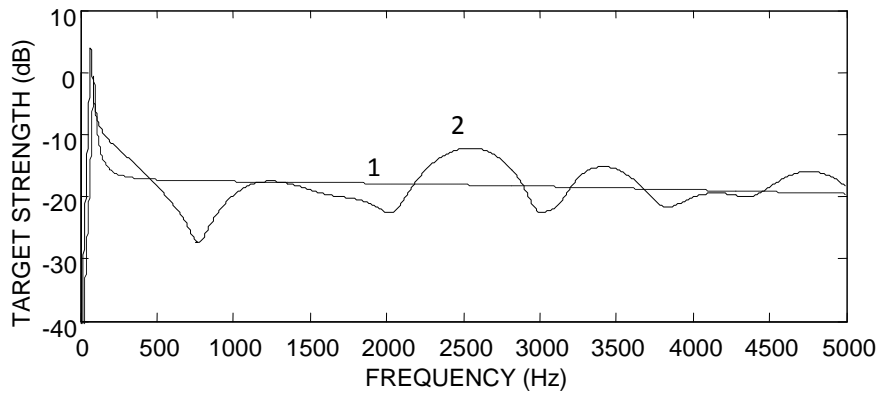
Figure 6: Effect of different deviations of fish locations. The deviation is gradually increased: (a)$\sigma = 4$ cm; (b)$\sigma = 8$ cm; (c)$\sigma = 16$ cm. The fish spacing is maintained at $d = 60$ cm. Line 1 is for incoherent summation; line 2 is for the self consistent model.

Figure 6 shows the effect of different deviations on the school scattering behavior. The variability is changed from 4 to 16 cm but the spacing is all at 60 cm. These three figures indicate that at low frequency target strength is relatively unchanged under different deviations, but it will begin to smooth out at the high-frequency by increasing the deviation. This phenomenon can show the effect of the schooling structure on the scattering behavior. When the deviation is 4 cm in (a), this is corresponding to a school with an order structure and the scattering is sensitive to the frequency; conversely, at $\sigma = 16$ cm, the school is loose and disorder, then the multiple scattering is not so important.

2.2 Averaging

The output of the echo-sounder is *rawdata*, normally including many pings and they needs to be averaged for further analysis. This can be achieved by the following equation (Baisgård, M., 2008):

$$p_{avg}[n] = \frac{1}{M} \sum_{m=0}^{M-1} p[m, n] \tag{21}$$

where *p* is power, *n = 0, 1...N -1* represents samples per ping and *0 < m < M -1* represents pings.

3 Acoustic experiment and data acquisition

3.1 Experiment site and the harvesting operation

The experiment was conducted at Innovamar, which is a plant for the landing, harvesting and processing of farmed salmon (Figure 7) on April, 18th. The harvesting operation was started at around 0430 am and lasted for 8-10 hours to finish one cage.

The daily operation of the plant is shown by Figure 8. Firstly one well boat with salmon will come to the cage and transfer the salmon into the cage by a pipe (Figure 8 (a)). The dimension of one cage is $24 \times 24 \times 15\,\text{m}$ and separated into 4 parts. The main components are netting, pump hose, lifting strain, rings, ropes and dead fish remove equipment. The pump intake at the depth of 1.5 meter has a diameter of 24 inches (609.6mm). Diameter of the pumping pipe itself is 350mm inner diameter. The electricity power of pump is 150 Kw (Figure 8 (b)). All nets are equipped with fixed rings mounted with 1 meter distance on lifting strain. Through these rings the lifting strain runs which gives all the rings free movement in both directions along the lifting strain. The fish will be guided toward the pumping inlet by raising the net from the opposite side of the farm (Figure 8 (c)). The interval of this process depends on the total fish which need to be harvested and the size of the fish, normally around 2 hours. For an 8 hours operation, the crowding net should be raised for 3-4 times.

After finishing the crowding, the pumping is started (Figure 8 (d)). The netting is lifted up by hand to reduce the volume and increase the fish density and guide the fish toward the pump intake. This step becomes frequent near the end of the harvesting (Figure 8(e)). An electronic display near the farm can show the number of fish passing through the main pipe into the process facility per minute. The number is maintained between 150 and 200. This can be used to roughly control pumping speed.

(a) The cages

(b) The process factory

Figure 7: Overview of the Innovamar plant

(a) Well boat: fish are transferred from well boat into the plant through a pipe.

(b) One cage.

(c) Crowding the fish by raising the net

(d) Finish the crowding and start pumping

(e) Lift up the net from the side by hand and guide the fish into the pump near the end of the harvesting.

(f) One electronic board displays the number of fish per minute passing through the main pipe.

Figure 8: The procedure of the harvesting operation

3.2 Experiment materials

1) Simrad science echo sounder EK15

Two single-beam echo-sounders have been applied in this experiment to collect the acoustic backscattering data of the fish school near the pump-intake. The main performance specifications are shown in Table 2. The experiment focused on the relatively changing of the backscattering strength rather than the exact value, therefore the calibration was not conducted.

Table 2: Performance specifications for Simrad EK15 single beam transducers.

Frequency (kHz)	200
Pulse duration (μs)	80
Ping rate (Hz)	40
Ping interval (ms)	500
Output power (W)	45
Beamwidth (Degree)	26
Bandwidth (Hz)	3088

2) Wooden plates:

Two wooden flat plates have been designed for holding the two transducers and collecting the acoustic data at certain ranges. The dimension of the plate is 1X1.2X0.010 m; make a hole with the diameter of 29mm at the center of the plate to place the transducer and two smaller holes at the top of the board for ropes; in order to keep the plate underwater, weight is added at the hole at the middle of the bottom (Figure. 9).

Figure 9: One wooden plate for holding the transducer.

3.3 Experiment setup

As shown in Figure 10, two plates carrying two transducers are fastened to two ropes (Rope 1 and Rope 2), which are at a same height. The position of transducer 1 is fixed, while the position of transducer 2 is controlled by Rope 3 and rings. Rope 4 is used to maintain the plate 2 in the vertical direction.
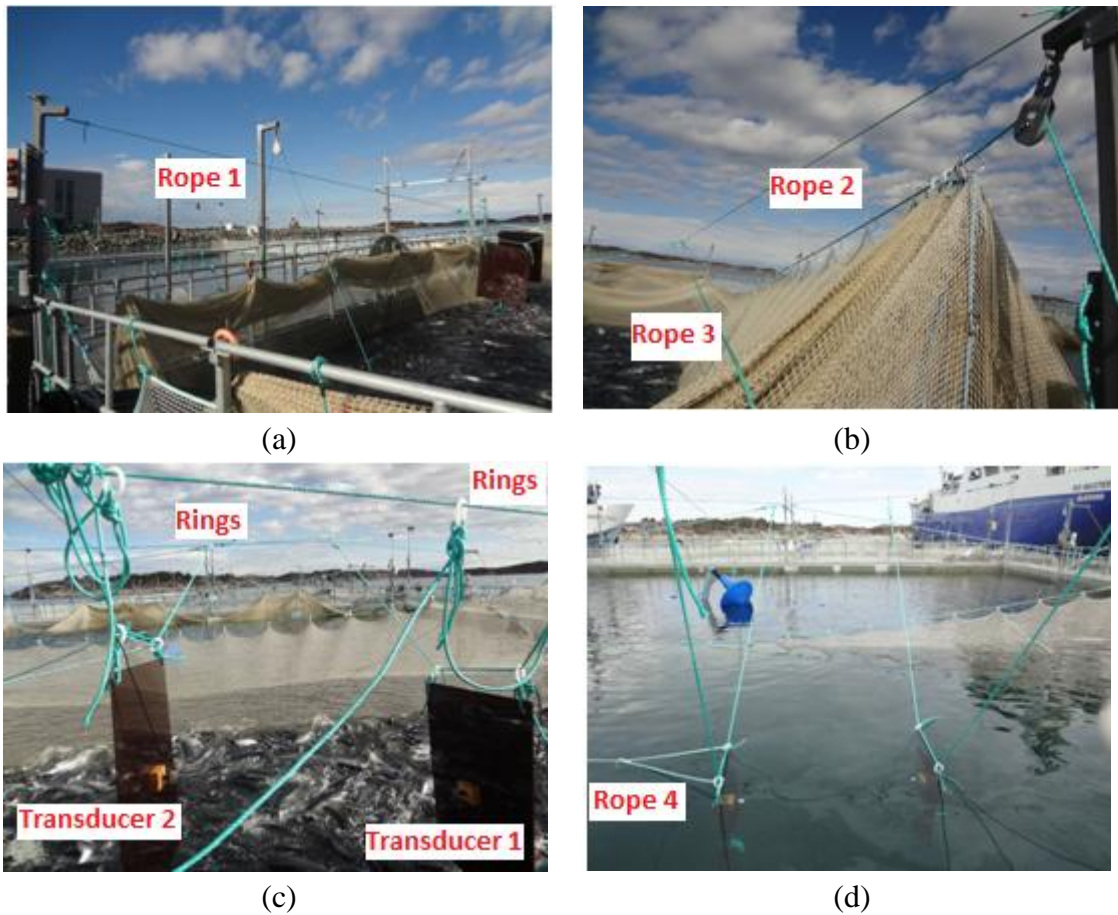
Figure 10: Experiment setup

3.4 Experiment results

The average weight of the salmon on this badge is 5.7kg with the proximate length of 78-83cm. The harvesting in the first crowding started from 0840 to 1100; the biomass harvested is 49921kg. The harvesting in the second crowding started from 1130 to 1315; the biomass harvested is 70418kg.

The process of the experiment is shown in Table 3. The experiment consisted of two parts (normal group and control group); the normal group was conducted during the harvesting and the control group was done after the harvesting with few free fish inside the net. The distance between 2 plates was changed from 4 to 3, 2. 5 and 1.5m within each group (Figures 11 and 12).

As mentioned in Figure 8, during the normal harvesting, the continuous pumping will reduce the fish density; however, it will be increased again by lifting up the netting by hands. It is hard to quantify how the manual acting will affect the density.

The raw data recorded by the echo-sounders will be processed with Matlab. The power data with no TVG function is chosen for the further analysis as shown in chapter 4.

Table 3: Overview of the process of the experiment.

Distance	Start time	End time	Ping No.	Note
Normal group: for the 1st crowding period				
1st 4m	0856	0905	101	
1st 3m	0907	0913	86	
1st 2.5m	0916	0933	219	
1st 1.5m	0935	0939	58	
2nd 4m	0948	0953	58	
2nd 3m	0954	1000	81	
2nd 2.5m	1002	1007	55	
2nd 1.5m	1009	1014	60	
3rd 4m	1018	1022	51	Lifted up the net
3rd 3m	1023	1028	56	Lifted up the net
3rd 2.5m	1029	1034	62	lifted up the net
3rd 1.5m	1040	1044	46	
Normal group: for the 2nd crowding period				
1st 4m	1151	1158	94	Lifted up the net
1st 3m	1202	1209	85	Lifted up the net
1st 2.5m	1211	1218	79	
1st 1.5m	1221	1225	26	Lifted up the net
2nd 4m	1228	1233	33	Lifted up the net
2nd 3m	1235	1240	35	
2nd 2.5m	1243	1248	39	Lifted up the net
2nd 1.5m	1252	1258	44	Lifted up the net
Control group: Nearly empty cage with few fish				
1.5	1341	1344	31	
2.5	1348	1349	4	
3	1350	1351	4	
4	1352	1353	7	
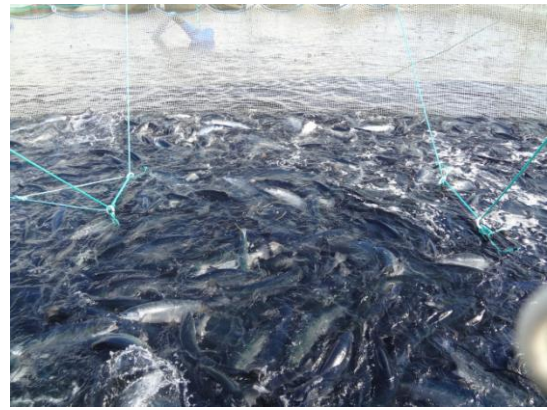
(a) 4m	(b) 3m
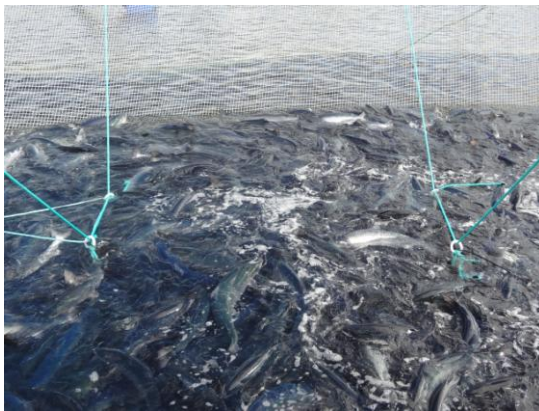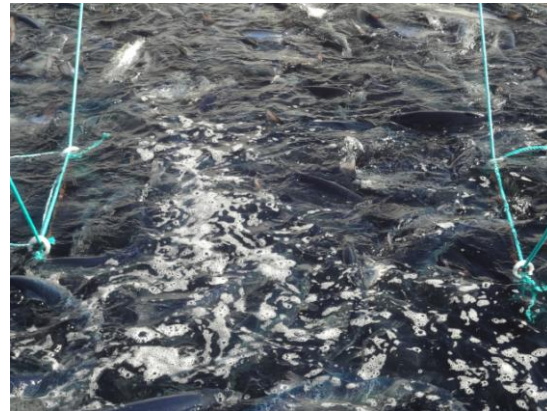
(c) 2.5m	(d) 1.5m.

Figure 11: The normal group conducted during the harvesting period: when the distance between the boards is (a) 4m; (b) 3m; (c) 2.5m and (d) 1.5m.

Figure 12: The control group conducted after the harvesting with few fish in the cage: the distance between the boards is set as 4m; 3m; 2.5m; 1.5m.

4 Results

4.1 Comparisons of power for single transducer within single crowding

In order to check how the backscattering strength of the fish school will be changed during the harvesting operation, the power data from a single transducer are compared when the distance between the plates is set as 4m, 3m, 2.5m, and 1.5m, respectively.

4.1.1 The 4m group in the 1st crowding
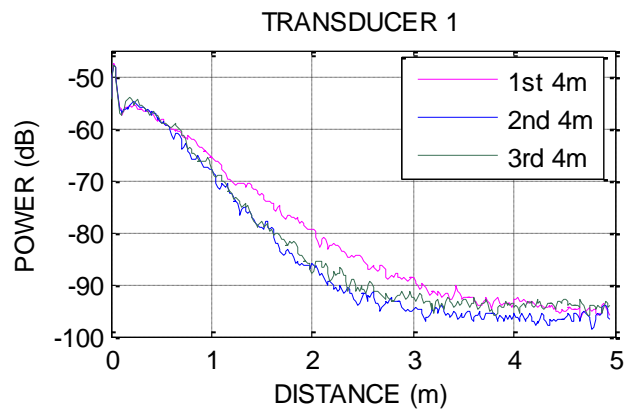
(a)
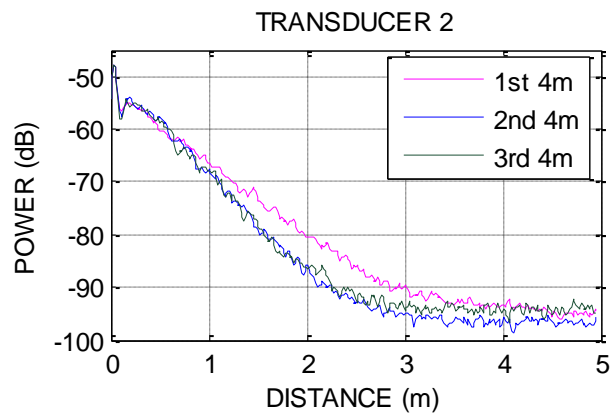
(b)

Figure 13: Measurement of the power in dB for (a) transducer 1 and (b) transducer 2 when the distance between plates is 4m in the 1st crowding.

Figure 13 shows the measurement of power in dB for (a) transducer 1 and (b) transducer 2 when the distance between plates is 4m in the 1st crowding.

From transducer 1, the power is decreased almost linearly from around -55 to -90dB at the distance from 0.2 to 2.5m, and then become stable at around -94dB at the distance from 2.5 to 5m for all three groups.

There is no significant difference between the results from the 2nd and 3rd group along the whole distance, while from the distance of 0.5 to 3.5m, the data from the 1st group is greater than the other two for about 5dB. All the three groups are not able to show the presence of the plates at 4m. The situation for transducer 2 is almost similar with transducer 1.

4.1.2 The 3m group in the 1st crowding

TRANSDUCER 1

(a)

TRANSDUCER 2

(b)

Figure 14: Measurement of power in dB from (a) transducer 1 and (b) transducer 2 when the distance between plates is 3m in the 1st crowding.

Figure 14 shows the measurement of power in dB for (a) transducer 1 and (b) transducer 2 when the distance between plates is 3m in the 1st crowding. From transducer 1, the power is decreased gradually from around -55 to -90dB at the distance from 0.2 to 3m, and then become stable at around -95dB at the distance from 3to 5m for all three groups. There is no significant difference between the results from the 1st and 2nd group along the whole distance, while from the distance of 1 to 3 m, the data from the 3rd group is smaller than the other two for about 5dB. All the three groups are not able to show the presence of the plates at 3m. The situation for transducer 2 is almost similar with transducer 1.

4.1.3 The 2.5m group in the 1st crowding

TRANSDUCER 1

(a)

TRANSDUCER 2

(b)

Figure 15: Measurement of power in dB for (a) transducer 1 and (b) transducer 2 when the distance between plates is 2.5m in the 1st crowding.

Figure 15 shows the measurement of power in dB for (a) transducer 1 and (b) transducer 2 when the distance between plates is 2.5m in the 1st crowding. From transducer 1, the power is decreased almost linearly from around -55 to -90dB at the distance from 0.2 to 2.6m, and then become stable at around -94dB at the distance from 2.6 to 5m for all three groups. There is no significant difference between the results from the 1st and 2nd group along the whole distance, while from the distance of 1 to 2.6 m, the data from the 3rd group is smaller than the other two for about 5dB. All the three groups are not able to show the presence of the plates at 2.5m. The situation for transducer 2 is almost similar with transducer 1.

4.1.4 The 1.5m group in the 1st crowding
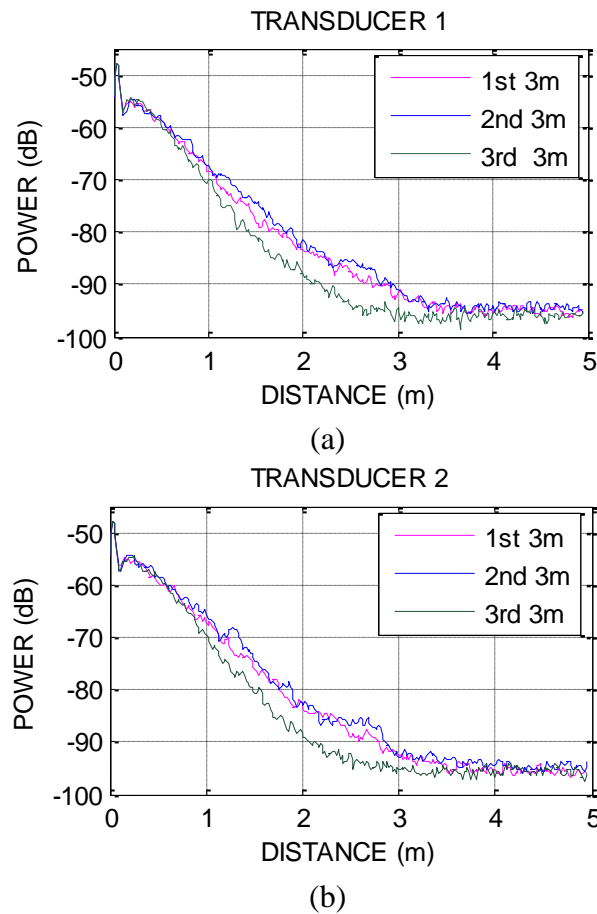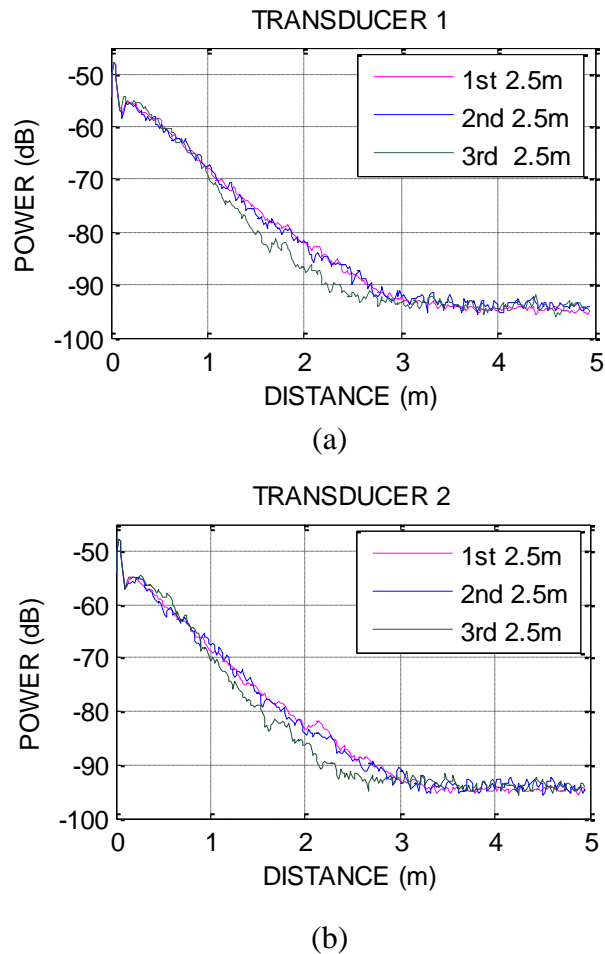
TRANSDUCER 1

(a)

TRANSDUCER 2

(b)

Figure 16: Measurement of power in dB for (a) transducer 1 and (b) transducer 2 when the distance between plates is 1.5m in the 1st crowding.

Figure 16 shows the measurement of power in dB for (a) transducer 1 and (b) transducer 2 when the distance between plates is 1.5m in the 1st crowding. From transducer 1, the power is decreased almost linearly from around -55 to -92dB at the distance from 0.2 to 2.7m, and then become stable at around -95dB at the distance from 2.7 to 5m for all three groups. There is no significant difference for the three groups from 0.2 to 1m and 2.7 to 5m; while from 1.6 to 2.7 m, the data from the 1st group is much greater than that from the 2nd group, and the 3rd group is the least. All the three groups are able to show the presence of the plates at around 1.5m. The situation for transducer 2 is almost similar with transducer 1.

4.1.5 The 4m group in the 2nd crowding

TRANSDUCER 1

TRANSDUCER 2

(a)

(b)

Figure 17: Measurement of power in dB for (a) transducer 1 and (b) transducer 2 when the distance between plates is 4m in the 2nd crowding.

Figure 17 shows the measurement of power in dB for (a) transducer 1 and (b) transducer 2 when the distance between plates is 4m in the 2nd crowding. From the two transducers, the power is decreased from around -55 to -90dB at the distance from 0.2 to 2.6m, and then become stable at around -92dB at the distance from 2.6 to 5m for all two groups. All the two transducers are not able to show the presence of the plates at 4m. For the transducer1, there is no significant difference for the three groups from 0.2 to 1m and 3.5 to 5m; while from 1 to 3.5 m, the data from the 1st group is much greater than that from the 2nd group for around 2dB. From transducer 2, the data for the two groups is similar from 0.2 to 2.3m, while the 2nd group is larger than the 1st group from 2.3 to 5m.
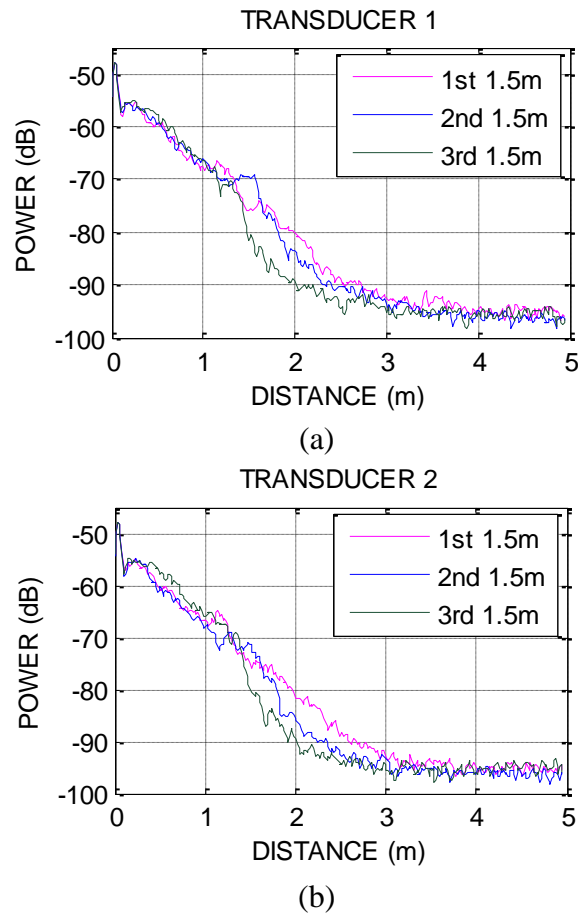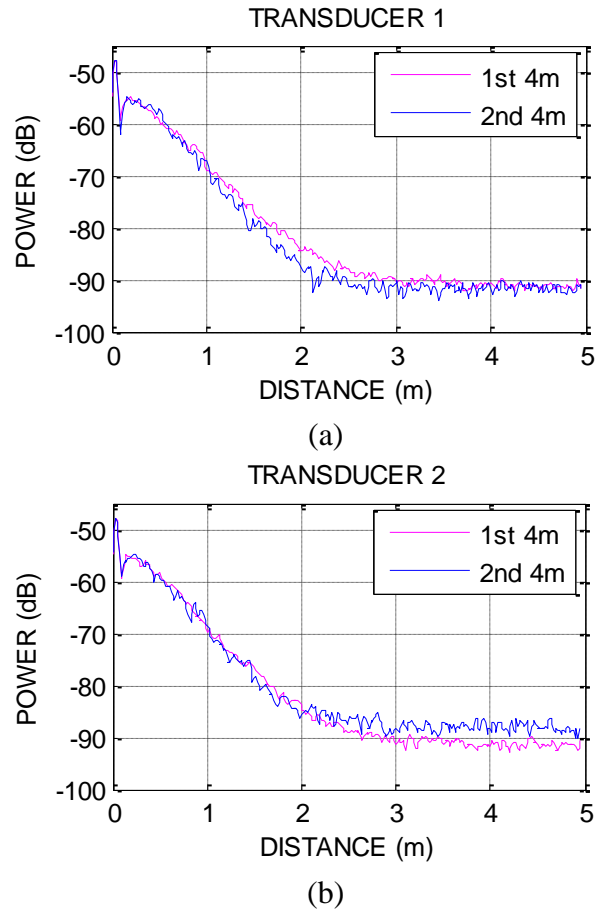
4.1.5 The 4m group in the 2nd crowding

Figure 17: Measurement of power in dB for (a) transducer 1 and (b) transducer 2 when the distance between plates is 4m in the 2nd crowding.

Figure 17 shows the measurement of power in dB for (a) transducer 1 and (b) transducer 2 when the distance between plates is 4m in the 2nd crowding. From the two transducers, the power is decreased from around -55 to -90dB at the distance from 0.2 to 2.6m, and then become stable at around -92dB at the distance from 2.6 to 5m for all two groups. All the two transducers are not able to show the presence of the plates at 4m. For the transducer1, there is no significant difference for the three groups from 0.2 to 1m and 3.5 to 5m; while from 1 to 3.5 m, the data from the 1st group is much greater than that from the 2nd group for around 2dB. From transducer 2, the data for the two groups is similar from 0.2 to 2.3m, while the 2nd group is larger than the 1st group from 2.3 to 5m.

4.1.6 The 3m group in the 2nd crowding

TRANSDUCER 1

(a)

TRANSDUCER 2

(b)

Figure 18: Measurement of power in dB for (a) transducer 1 and (b) transducer 2 when the distance between plates is 3m in the 2nd crowding.

Figure 18 shows the measurement of power in dB for (a) transducer 1 and (b) transducer 2 when the distance between plates is 3m in the 2nd crowding. From transducer 1, the power is decreased from around -55 to -89dB at the distance from 0.2 to 2.5m, and then become stable at around -89dB at the distance from 2.6 to 5m for the 1st group; the distribution of the power for the 2nd group is similar with the 1st one but higher for around 3dB. From transducer 2, the data for the two groups is almost the same along the whole distance. All the two transducers are not able to show the presence of the plates at 3m.

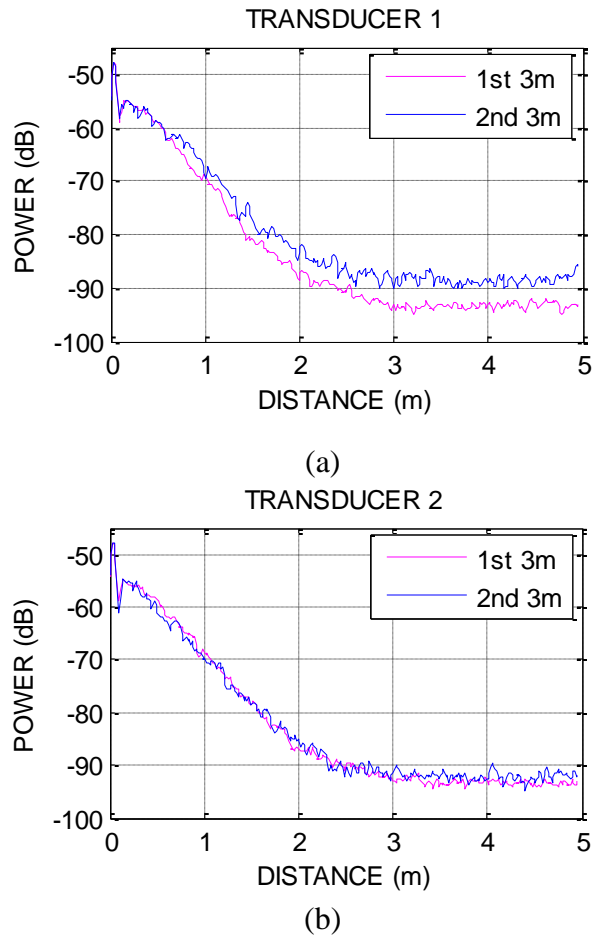**4.1.7 The 2.5m group in the 2nd crowding**

(a)

(b)

Figure 19: Measurement of power in dB for (a) transducer 1 and (b) transducer 2 when the distance between plates is 2.5m in the 2nd crowding.

Figure 19 shows the measurement of power in dB for (a) transducer 1 and (b) transducer 2 when the distance between plates is 2.5m in the 2nd crowding. From the 1st group of transducer 1, the power is decreased from around -55 to -95dB at the distance from 0.2 to 2.5m, and then become stable at around -95dB at the distance from 2.5 to 5m; for the 2nd group, the power is decreased from around -55 to -85dB at the distance from 0.2 to 2.5m, and then become stable at around -90dB at the distance from 2.5 to 5m. The situation is similar for transducer 2. All the two transducers are not able to show the presence of the plates at 2.5m.
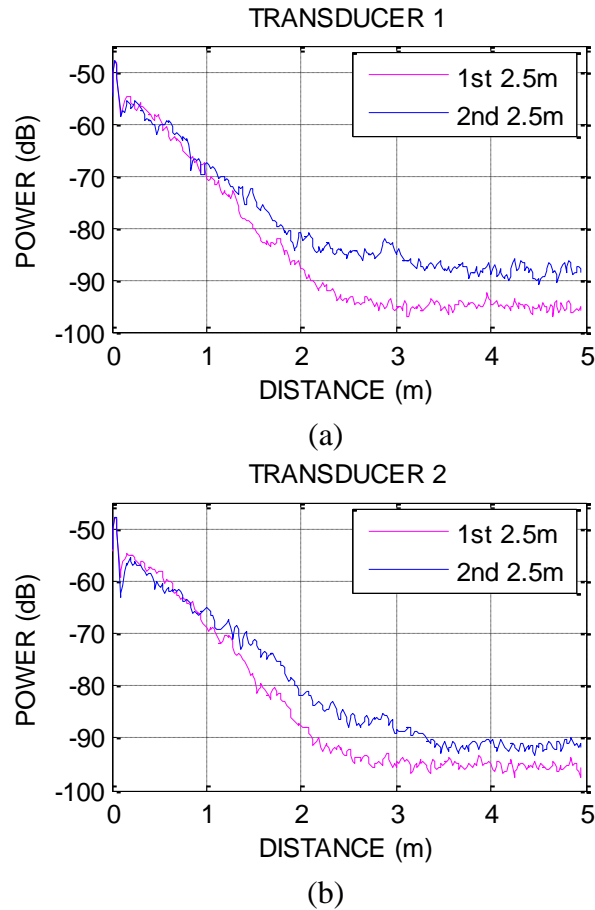
4.1.8 The 1.5m group in the 2nd crowding

(a)

(b)
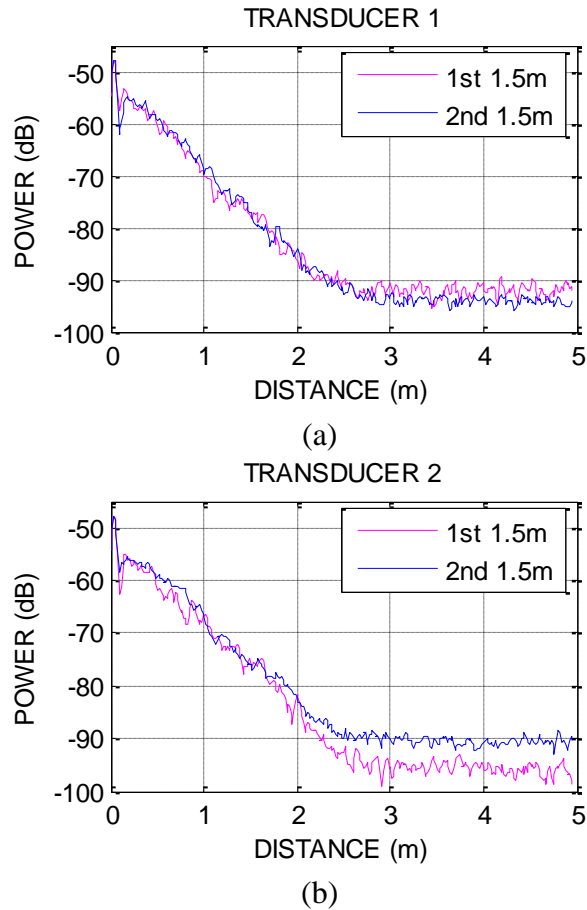
Figure 20: Measurement of power in dB for (a) transducer 1 and (b) transducer 2 when the distance between plates is 1.5m in the 2nd crowding.

Figure 20 shows the measurement of power in dB for (a) transducer 1 and (b) transducer 2 when the distance between plates is 1.5m in the 2nd crowding. The power is decreased from around -55 to -92dB at the distance from 0.2 to 2.5m for all groups from two transducers. From 2.5 to 5m, the power for the 1st group is little higher than that for the 2nd from transducer 1; the opposite situation occurs at the transducer 2. All the two transducers are not able to show the presence of the plates at 1.5m.

4.1.9 Summary

For both two crowding periods, the trends of the distribution of power on the distance are very similar. The power is reduced from around -50dB at 0.2m to around -70dB at near 1m, and then -90dB at near 2.5m. As the distance is further increased, the power becomes stable at around -93dB. The plates are only found in the 1.5m group of the 1st crowding period.

These can be explained by that the fish density near the two transducers is really high. The acoustic energy is attenuated rapidly within a short distance and the scattering strength from the plates and the fish in distant is very weak.

The data for the two transducers are almost the same. It might be resulting from the uniform distribution of the fish density inside the netting.

4.2 Comparisons of noised reduced power for two transducers and two crowding operations

Based on the results from 4.1, the data from the two transducers are almost the same. So in this section, an average of the powers of Transducer1 and Transducer 2 at the first, second and third time from the two different crowding will be used.

As found in Table 3, the 1st and 2nd group data have 4 components from both two crowding. For instance, in the 4m group (Figure 21), power data for the 1st4m is averaged from Transducer1 and Transducer 2 at the 1st4m during the 1st crowding period, and Transducer1 and Transducer 2 at the 1st4m during the 2nd crowding period; power data for the 2nd 4m is averaged from Transducer1 and Transducer 2 at the 2nd 4m during the 1st crowding period, and Transducer1 and Transducer 2 at the 2nd 4m during the 2nd crowding period; power data for the 3rd4m is averaged from Transducer1 and Transducer 2 at the 3rd 4m during the 1st crowding period.

4.2.1 The 4m group

Figure 21: Noise-reduced power for 4m.

When the distance between the plates is 4m (Figure 21), for the 1st group, the power is decreased from around -55 to -90dB when the distance is increased from 0.2 to 3m; and then become stable at around -93dB when the distance is from 3 to 5m.
The results for the 2nd group and the 3rd group are similar, and they are lower than the 1st group between 1 to 3.5m for around 4dB.

4.2.2 The 3m group

Figure 22: Noise-reduced power for 3m.

When the distance between the plates is 3m (Figure 22), for the 1st group, the power is decreased from around -55 to -92dB when the distance is increased from 0.2 to 3m; and then become stable at around -94dB when the distance is from 3 to 5m.

The results for the 2nd group is higher than the 1st group for around 2dB when the distance is larger than 1m; while the 3rd group is much lower than the 1st group for around 3dB.
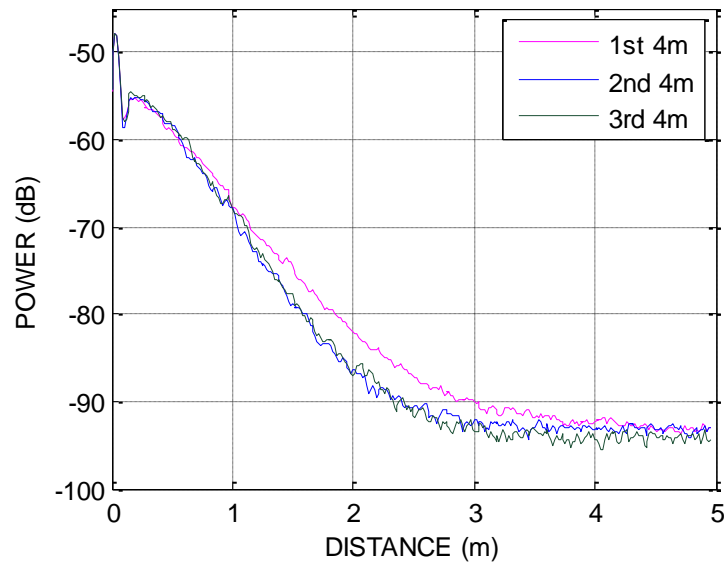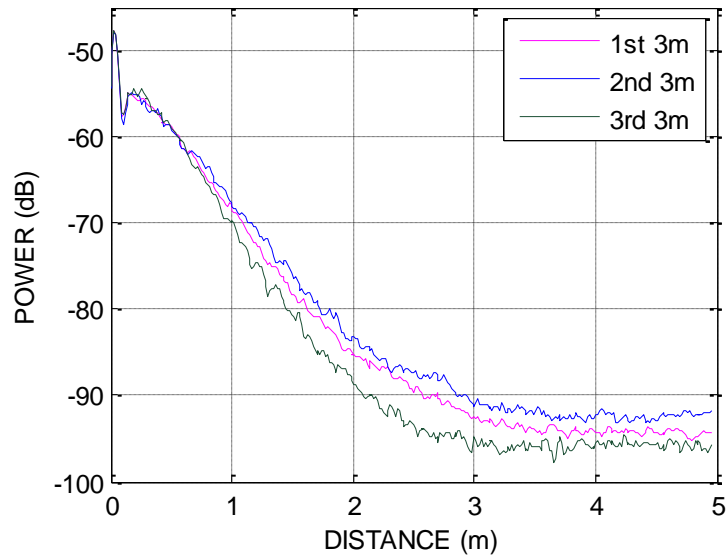
4.2.3 The 2.5m group
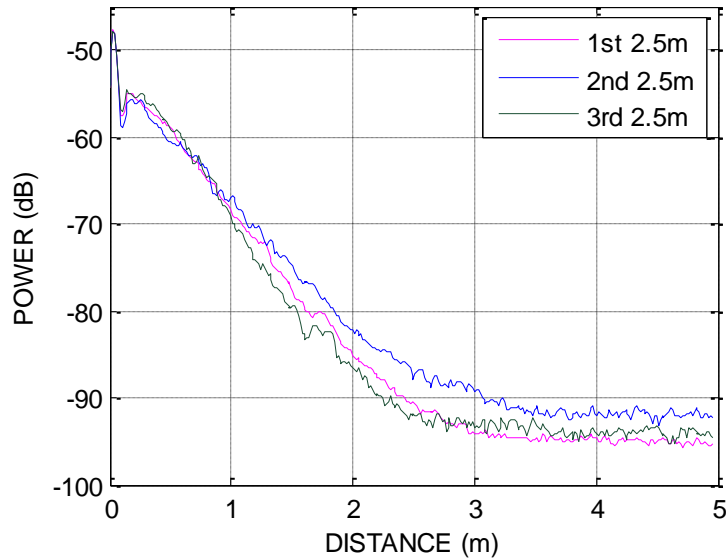
Figure 23: Noise-reduced power for 2.5m.

When the distance between the plates is 2.5m (Figure 23), for the 1st group, the power is decreased from around -55 to -91dB when the distance is increased from 0.2 to 2.5m; and then become stable at around -95dB when the distance is from 2.5 to 5m.

The results for the 2nd group is higher than the 1st group for around 3dB when the distance is larger than 1m; while the 3rd group is lower than the 1st group for around 2dB between 1 to 3m.

4.2.4 The 1.5m group
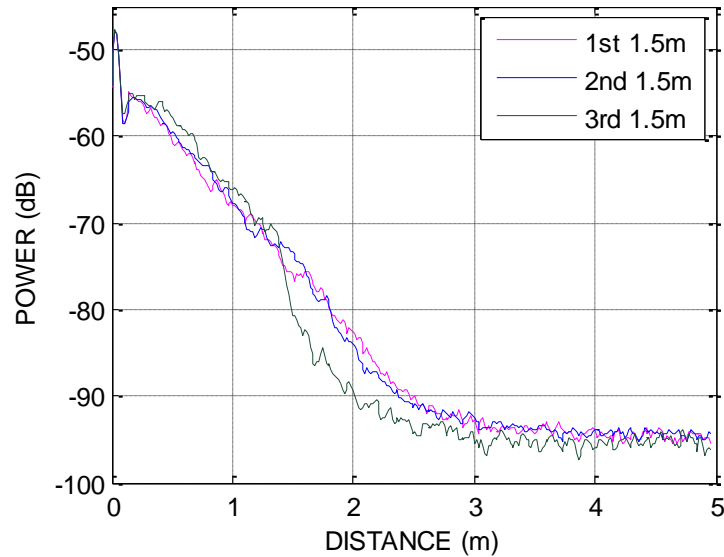
Figure 24: Noise-reduced power for 1.5m.

When the distance between the plates is 1.5m (Figure 24), the data from the 1st group and the 2nd group is similar along the whole distance: decreased from -55 to -91dB when the distance is changed from 0.2 to 2.5m, and then be stable at around -94dB.

The data from the 3rd group is lower than the other two about 10dB between 1.5 to 2.5m.

4.2.5 Summary

The 3rd group data for the four different distances are lower than the other two groups. This phenomenon can be explained by three reasons, as reported in table 3.2: (1) for the 1st crowding, fish biomass in the cage has been great reduced by the pump; (2) for the 1st crowding, netting is never raised up before the 3rd group; (3) for the 2nd crowding, the netting has been raised a lot for both two groups. All these factors may lead to higher average value of power at the 1st and 2nd groups than the 3rd.

4.3 Comparisons of power from nearly empty cage (control group)

TRANSDUCER 1

(a)

TRANSDUCER 2

(b)

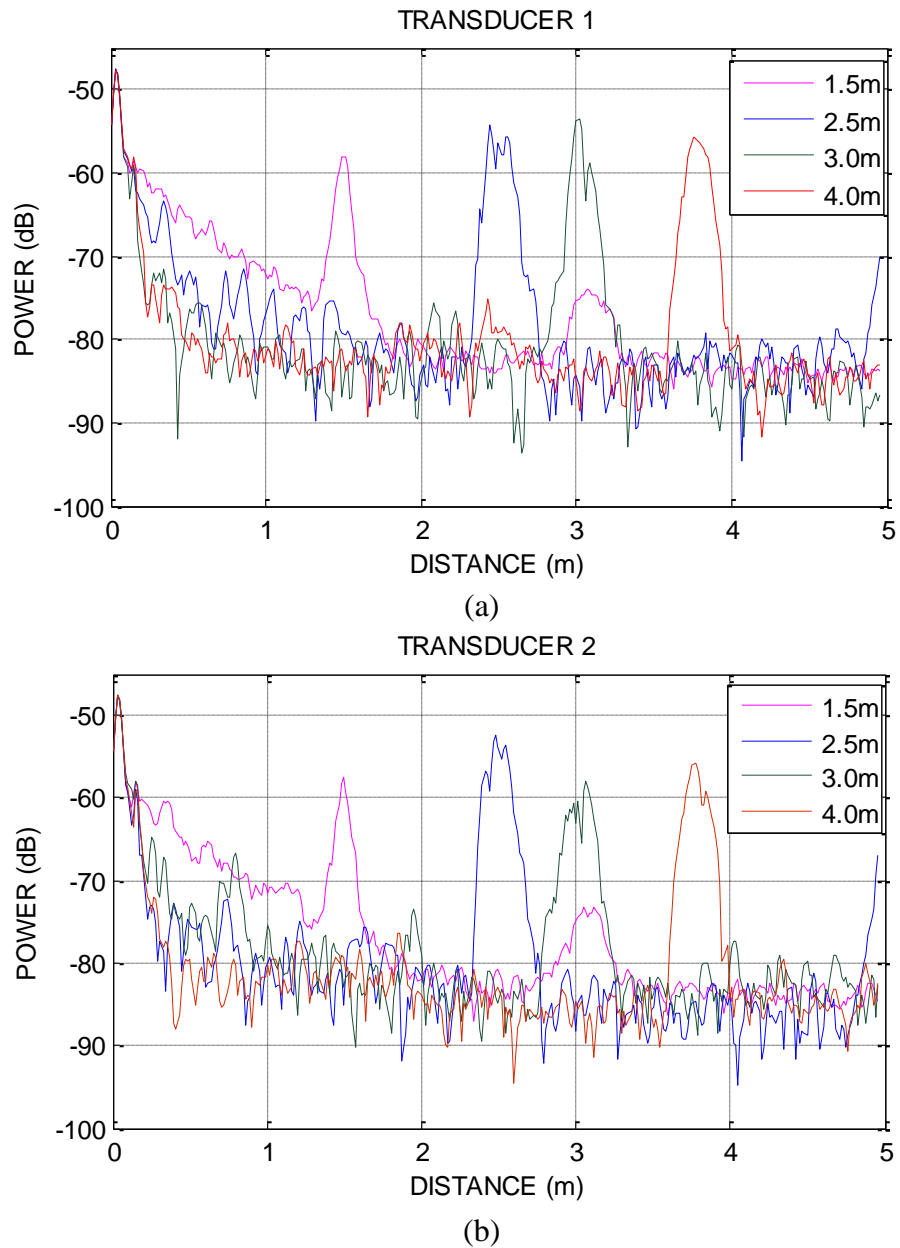Figure 25: Measurement of power in dB for (a) transducer 1 and (b) transducer 2 in the control group when the distance between the plates is 1.5m (pink line); 2.5m (blue line); 3.0m (green line) and 4.0m (red line).

One measurement has been conducted as a control group after the harvesting in the nearly empty cage with few fish, as show in figure 25. The distance between the plates is set as 1.5m, 2.5m, 3m and 4m, respectively.

The power of the four different distance groups starts with -58dB at 0.2m, and then gradually is reduced to around -80dB at 1m, and finally becomes stable in the longer distance, except for the peaks.

From transducer 1, when the distance between the plates is 1.5m, there is one clear peak at 1.5m with a value of -58dB; when the distance is changed into 2.5m, a peak appears at 2.5m with a value of -54dB; in the 3.0m group, one peak appears at 3.0m with a value of -54dB; for the 4.0m group, one peak appears at 3.75m with a value of -56dB.

When comparing figure 25 (a) and (b), the data from the two transducers have the same distribution along the whole distance for the four different groups.

These can be explained by that some fish pass by the transducer, which leads to the high power value in a short distance, while for the whole sample fish density is really low, so the position of the plates can be found clearly and the power can keep stable for a long distance.

4.4 Comparisons of averaged power from the normal group and control group

As reported by Foote (1987), shadow effect is a non-linearity behavior that occurs when measuring the scattering strength for a fish school with a really high density. Most of the acoustic energy transmitted is attenuated by the fish near the transducer, thus the distant fish would reflect less signal.

In order to show how the shadow effect has an effect on the received backscattering strength, the averaged power from the normal group is compared with the control group. The results are shown in figure 26 to 29.

Some features can be found from the normal group and control group for all four different distance groups: firstly, there is no peak value near the positions of the plates for the normal group, while the control group has a clear one; secondly, at the range of 0.2m to 5m, the power of the control group is almost stable at -85dB, while the result of normal group is decreased rapidly at the distance between 0.2 and 2.6m; finally the result from the normal group becomes lower than that from the control group when the distance is greater than 1.8m.

When compared to the real distribution of fish density in figure 3.5, the power from the normal group is non-linearly and rapidly reduced. This may be explained by two potential reasons: the shadow effect and multiple scattering caused by the extremely high fish density in the sample volume. The shadow effect is more important in this experiment.

Figure 26: Comparison for the averaged power in dB from the normal group and control group when the distance between the plates is 4m.

Figure 27: Comparison for the averaged power in dB from the normal group and control group when the distance between the plates is 3m.
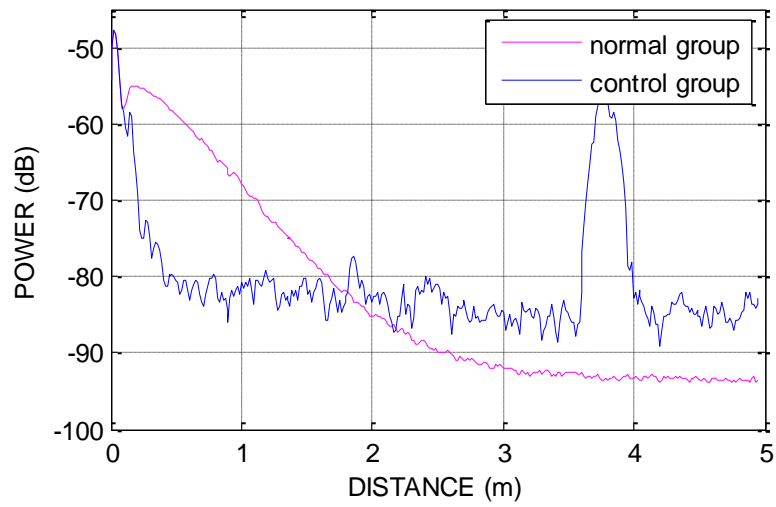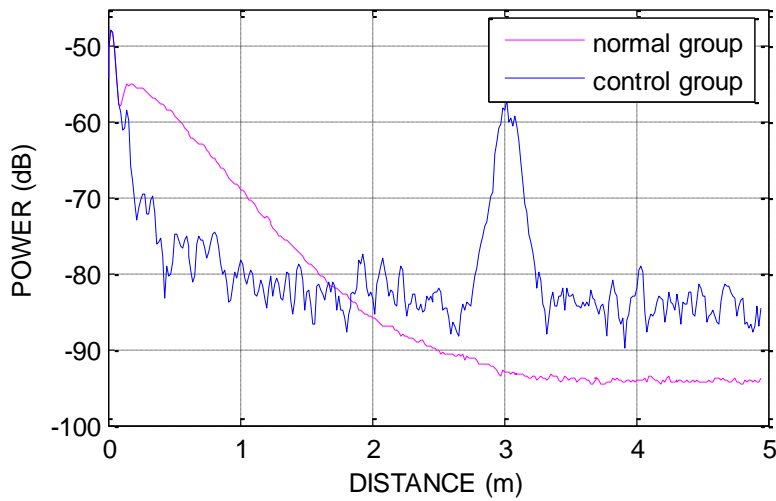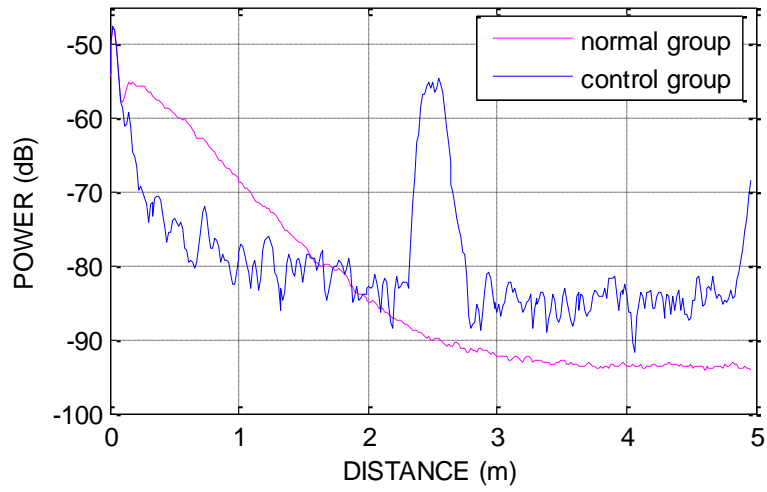
Figure 28: Comparison for the averaged power in dB from the normal group and control group when the distance between the plates is 2.5m.
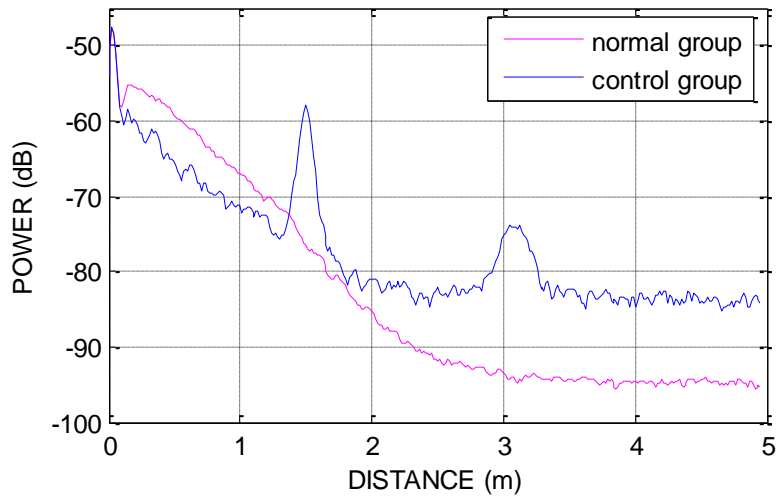

Figure 29: Comparison for the averaged power in dB from the normal group and control group when the distance between the plates is 1.5m.

5 Discussions and future work

The time for this experiment is so short and the collected data is limited. Many things could be improved in the further study:

- The time of each data file is different and this might be impact the averaged data. It is better to keep them the same in future.

- The main goal of this experiment is to check if the transducer is sensitivity to the changed fish density and not to find the exact value of the fish density, the transducers applied here was not calibrilated. It would be necessary to perform the calibration according to the standard method in the next step, so the data will be more rigorous. More control experiments could be done with single fish and few fish and their results can be used as the reference in the later analysis for the normal group.

- The fish density is really high during the harvesting and the plate used to evaluate the shadow effect cannot be found from most of the groups. The power is rapidly reduced within 3m. So the plate might be changed into few small metal spheres with certain given sizes. They can be distributed in front of the transducer with a distance around 0.4 to 3m and then more information for the attenuation of acoustic energy might be get at different range.

- Power is chosen in the report to analyze the backscattering feature of fish school instead of volume scattering strength. Because the fish density is too high to apply 20log time-varied gain (TVG) to compensate for the absorption losses and spreading. While the power data couldn't be connected with the fish density or biomass directly. It will be very interesting to find a proper TVG for this situation.

- The real fish density inside the netting is control by the total biomass at the beginning of the harvesting, the pumping speed and the lifting up operation by hand. The first two factors should be recorded. It is impossible to quantify the lifting up operation accurately. This is corresponding to the reduced of the netting depth. If the depth of the netting can be estimated, then the approximate volume of the netting could be calculated. A better estimation of the real fish density can be get and then compared it with the acoustic results, the final results will more reliable.

6 Conclusions

Acoustic method was applied to detect if the sensitivity of the echo sounder is feasible for density estimation. The experiment was conducted at the Salmar Innovamar harvesting and processing plant with two Simrad EK15. Raw data from the echo sounder was processed by Matlab to get the power data without range compensation.

Some of the acoustic results can be explained with the harvesting operation. When comparing the power data from a single transducer, it can be found that all groups have similar trends along the whole distance. Due to the high density, the power is reduced rapidly within a range of 2m; especially from 0.2 to 1m, the power value is almost the same for all groups. The plates are only found in the 1.5m group of the 1st crowding period. Since the distribution of power is nearly similar for the two transducers, the power of Transducer1 and 2 is averaged to get a noised reduced power. From the noise reduced power, it could be found that the 3rd group data from all the four different distances are clearly lower than the 1st and the 2nd group. The reasons can be found when comparing with the real harvesting operation. During the 1st crowding period, the netting is seldom raised before the 3rd group, while it is lifted up frequently for the both two groups during the 2nd crowding period.

In order to show how the shadow effect will affect the backscattering strength, one control group inside a nearly empty cage is done after the normal harvesting. For the control groups, peaks near the positions of plates could be found clearly and the distribution of the power along the distance is almost stable. This is because that fish density is really low and the attenuation of acoustic energy is quite weak. Further comparing the results from the control group with the average power from the normal group, it can be found that the data of the normal group are much lower than that of the control group when the distance is greater than 1.8m. But the real fish density in the normal group is much higher than the control group. This confirms that the fish density in the normal operation is very high. So we could not connect the power data with fish density directly in this report, but this experiment could provide some information about the acoustic scattering from high fish density in aquaculture for the further study.

References

Alvarez, A., Ye, Z. 1999. Effects of fish school structures on acoustic scattering. ICES Journal of Marine Science, 56: 361–369.

Azzali, M., Leonori, I., Biagiotti,I. *et al.* 2010. Target strength studies on Antarctic Silverfish (*Pleuragramma antarcticum*) in the Ross Sea. CCAMLR Science, 17: 75–104.

Baisgård, M. 2008.Multi-frequency backscattering from the sea floor; can the frequency response be used to identify typical sandeel grounds? Norwegian University of Science and Technology, Department of Electronics and Telecommunications.

Clay, C.S., Horne, J.K. 1994. Acoustic models of fish: The Atlantic cod (*Gadus morhua*). J. Acoust.S oc. Am. 96 (3): 1661-1668.

Feuillade, C. 2001. Acoustically coupled gas bubbles in fluids: Time-domain phenomena. J. Acoust. Soc. Am. 109 (6): 2606- 2615.

Feuillade, C., Nero, R. W., Love, R.H. 1996. A low-frequency acoustic scattering model for small schools of fish. J. Acoust. Soc. Am. 99 (1): 196-208.

Foote, K.G.1980. Effect of fish behavior on echo energy: the need for measurements of the orientation distributions. Journal de Conseil international pour l'Exploration de la Mer, 39:193–201.

Foote, K, G., Francis, D.T.I. 2002. Comparing Kirchhoff-approximation and boundary-element models for computing gadoid target strengths. J. Acoust. Soc. Am. 111 (4): 1644-1654.

Gorska, N., Ona, E. 2003. Modelling the acoustic effect of swimbladder compression in herring. ICES Journal of Marine Science, 60: 548–554.

Gurshin, C. W. D., Jech, J. M., Howell, W. H., *et al*. 2009. Measurements of acoustic backscatter and density of captive Atlantic cod with synchronized 300-kHz multibeam and 120-kHz split-beam echosounders. – ICES Journal of Marine Science, 66: 1303–1309.

Hahn, T.R. 2007. Low frequency sound scattering from spherical assemblages of bubbles using effective medium theory. J. Acoust. Soc. Am. 122(6): 3252- 3267.

Hovem, J.M. 2012. Marine Acoustics-The Physics of Sound in Underwater Environments. Peninsula Publishing.

Kang, D., Hwang, D. 2003. *Ex situ* target strength of rockfish (*Sebastes schlegeli*) and red sea bream (*Pagrus major*) in the Northwest Pacific. ICES Journal of Marine Science, 60: 538–543.

Knudsena, F.R., Fosseidengen, J.E., Oppedal, F. *et, al*. 2004. Fisheries Research,69: 205–209.

Kubilius, R., Ona, E. 2012. Target strength and tilt-angle distribution of the lesser sandeel (*Ammodytes marinus*) ICES Journal of Marine Science, 69(6), 1099–1107.

Love, R.H. 1978. Resonance acoustic scattering by swimbladder-bearing fish. J. Acoust. Soc. Am. 64: 571-580.

Minnaert, M. 1933. On musical air-bubbles and the sounds of running water. Philos. Mag. 16: 235-248.

Puig,V., Espinosa, V., Soliveres,E. *et,al*. 2012. Biomass estimation of Bluefin Tuna in sea cages by the combined use of acoustic and optical techniques. Collect. Vol. Sci. Pap. ICCAT, 68(1): 284-290.

Reine, K., Clarke, D., Dickerson, C. et al. 2010. The Relationship Between Acoustic Target Strength and Body Length for Atlantic Sturgeon (*Acipenser oxyrinchus oxyrinchus*). ERDC TN-DOER-E27.

Simmonds, J., MacLennan, D. 2005. Fisheries Acoustics: Theory and Practice, 2nd edition. Blackwell, Oxford.

Twersky, V. 1962. Multiple scattering of waves and optical phenomena. J.Opt.Soc.Am. 52: 145- 171.

Ye , Z. , Farmer, D.M. 1996. Acoustic scattering by fish in the forward direction. ICES

Journal of Marine Science, 53: 249-252.

Zhao, X.Y., Ona, E.2003. Estimation and compensation models for the shadowing effect in dense fish aggregations. ICES Journal of Marine Science, 60: 155–163.

Website:

http://www.soundmetrics.com/products
http://www.salmar.no/About-SalMar/InnovaMar
Salmon Farming Industry Handbook 2012